Optimal Sensor Placement for State Reconstruction of Distributed Process Systems

Antonio A. Alonso
Process Engineering Group, IIM-CSIC, 36208 Vigo, Spain

Christos E. Frouzakis and Ioannis G. Kevrekidis
Dept. of Chemical Engineering, Princeton University, Princeton, NJ 08544

DOI 10.1002/aic.10121
Published online in Wiley InterScience (www.interscience.wiley.com).

In this contribution we propose a systematic approach to field reconstruction of distributed process systems from a limited and usually reduced number of measurements. The method exploits the time scale separation property of dissipative processes and concepts derived from principal angles between subspaces, to optimally placing a given number of sensors in the spatial domain. Basic ingredients of the approach include the identification of a low-dimensional subspace capturing most of the relevant dynamic features of the distributed system, and the solution of a max–min optimization problem through a guided search technique. The low-dimensional subspace can be defined either through a spectral basis (eigenfunctions of a linear or linearized part of the operator) or through a semiempirical expansion known in the engineering literature as the Proper Orthogonal Decomposition (POD) or Karhunen–Loeve expansion. For both cases, the optimal sensor placement problem will be solved by taking advantage of the underlying algebraic structure of the low-dimensional subspace. The implications of this approach for dynamic observer design will be discussed together with examples illustrating the proposed methodology. © 2004 American Institute of Chemical Engineers *AIChE J,* 50: 1438–1452, 2004

Keywords: distributed process systems, observer design, spectral decomposition, proper orthogonal decomposition, optimal sensor placement

Introduction

The operation and control of distributed process systems is often constrained by the cost and type of available sensors. In flow control, for instance, the fluid velocity field is available through only a limited number of fluid velocity sensors positioned at particular locations. In the case of chemical reactors, the measurement of chemical species concentrations is usually obtained by a small number of costly and slow chemical detectors. To guarantee reliable information for the control of such systems, efficient estimation schemes of the unobserved states, taking full advantage of the available information, are required. In this context, efficiency should be understood in the sense of *finding a small number of measurements that will provide a good estimation of the entire field of interest.*

Early approaches to field reconstruction in distributed process systems exploited results from dynamic linear systems theory to develop optimal state space observers through spatially discretized models of the system equations, such as finite differences or finite element methods (Alvarez et al., 1981; Harris et al., 1980; Kumar and Seinfeld, 1978; Windes et al., 1989). First, the original infinite dimensional system was approximated by a large number of ordinary differential equations describing the evolution of the relevant variables on a grid

Correspondence concerning this article should be addressed to A. A. Antonio at antonio@iim.csic.es.

of space positions. Estimation was then performed by minimizing a certain functional of the error between measurements at the proposed sensor locations and predictions obtained by the approximation at these positions. Sensors were placed so as to maintain the covariance matrix associated with the measurements well conditioned. Different criteria were used to that purpose, such as maximizing the trace or the covariance matrix determinant over a set of candidate locations. However, the search was done on a semiempirical basis without any general systematic method. Recent interesting alternatives include the maximization of measurement independence (Vande Wouweret al., 2000) or selection procedures guided by appropriate observability measures (van der Berget al., 2000). These alternatives, however, have been applied only to linear systems and/or to a small number of sensors.

Although the need for systematic methods for sensor placement was soon recognized (see, for example, Keller and Bonvin, 1992 and the review by Kubrusly and Malebranche, 1985), most techniques relied on an exhaustive search over a predefined set of candidate positions. This approach, although practical for a small number of degrees of freedom, proved to be unsuitable for systems requiring a high dimensional representation, such as in flow reconstruction (see, for example, Podvin and Lumley, 1998). Exceptions include a large-scale sequential measurement selection technique that, although suboptimal, was successfully applied in modal identification of large space structures (Kammer, 1991). Recently, Antoniades and Christofides (2001a) provided an elegant solution to the sensor placement problem through standard unconstrained optimization, by taking advantage of the time scale separation properties of reaction–diffusion systems under geometric control. The method is restricted, however, to a number of sensors equal to the dimension of the slow dynamics, and requires the system to be under a preestablished control scheme. More general situations, however, would demand sensor placement not to depend on a predetermined control structure, nor on a particular dynamic model because this could be poorly understood or unavailable. Under those circumstances, we propose a methodology that requires only the knowledge of a low-dimensional subspace capturing the most relevant features of the distributed process system state. Given this set (in our case, a hyperplane), the optimal sensor placement will be computed as that which minimizes the maximum angle between the low-dimensional hyperplane and the subspace of measurements (also a hyperplane), thus minimizing the error of the estimates. We also show that if a dynamic model of the process is available, the sensor arrangement obtained from the optimization of this criterion will also result in fast convergence dynamic observation schemes.

The structure of the low-dimensional subspaces (hyperplanes), and their relations with distributed process systems are described. The estimation approach is presented. We concentrate on the measurements selection problem (number of sensors and positions) and propose an algorithm to compute the optimal placement of a given number of sensors. Finally, the approach we suggest will be illustrated through two case studies involving linear diffusion and nonlinear reaction–diffusion systems.

Low-Dimensional Approximations of Distributed Process Systems

Let us consider the following quasi-linear partial differential equation

$$u_t = \mathcal{L}(u) + \sigma(u) \tag{1}$$

where $\mathcal{L}(\cdot)$ denotes a general linear parabolic operator defined on a (possibly 3-dimensional) spatial domain D with smooth boundary B and $\sigma(u)$ is a nonlinear function of u. The solution $u(x, t)$ in Eq. 1, with appropriate initial and boundary conditions, will be referred to as *the field* with $x = (x_1, x_2, x_3)^T$ denoting spatial coordinates. Equation 1 can be interpreted as an infinite dimensional system on a Hilbert space equipped with inner product and norm

$$\langle f, g\rangle = \int_D f(x)\, g(x) dx \qquad \|f\|_2^2 = \langle f, f\rangle$$

The solution of Eq. 1 can be represented in terms of an infinite series expansion of the form

$$u(x, t) = \sum_{j=1}^{\infty} c_j(t)\varphi_j(x)$$

In this expression, the coefficients c_j are functions of time, whereas the set of basis functions $\{\varphi_j(x)\}_{j=1}^{\infty} = 1$ contain the spatial dependency of the solution. Each element of this set can also be considered as the solution of the following integral equation

$$\varphi_j(x) = \mu_j \int_D \mathcal{K}(x, x')\varphi_j(x')dx' \tag{2}$$

where μ_j *i*s a parameter (eigenvalue) associated with each basis function φ_j. Under the orthonormality condition $\langle\varphi_i, \varphi_j\rangle = \delta_{ij}$, and depending on the nature of the kernel $\mathcal{K}(x, x')$, two different sets will be considered:

(1) *The spectral basis*, derived from a kernel $\mathcal{K}$ constructed as the Green's function associated with the spatial operator $\mathcal{L}(\cdot)$ (Courant and Hilbert, 1937). Each element of the set is called an eigenfunction and μ_j, its corresponding eigenvalue.

(2) *The POD* (*Proper Orthogonal Decomposition*) *basis* (Holmes et al., 1996), derived from the two-point correlation kernel

$$\mathcal{K}(x, x') = \frac{1}{\ell}\sum_{i=1}^{\ell} u(x, t_i)u(x', t_i) \tag{3}$$

where $u(x, t_i)$ is the value of the field at each instant t_i (snapshot), and the summation extends over a sufficiently large collection of snapshots $i = 1, \ldots, \ell$, which will be assumed representative of the dynamic behavior of the process. As it will become clear later on, the ordered structure of the ei-

genspectrum $\{\mu_j\}_{j=1}^{\infty}$ associated with this basis set will guide (for the case of low-dimensional dynamics) the selection of a finite low-dimensional basis $\{\varphi_j(x)\}_{j=1}^{k}$, which will capture the most relevant features of the solution. These features are then recovered by either projecting its solution at a given time or its defining Eq. 1 on the low-dimensional basis. In the static version, the solution is approximated as

$$\tilde{u} = \sum_{i=1}^{k} \langle u, \varphi_j \rangle \varphi_i(x) \tag{4}$$

In the dynamic version, Eq. 1 is projected on each element φ_i, so that

$$\langle u_t - \mathcal{L}(u) - \sigma(u), \varphi_j \rangle = 0$$

results in a set of ordinary differential equations of the form

$$c_t = Ac + f(c)$$

$$\tilde{u} = [\varphi_1, \ldots, \varphi_k]c \tag{5}$$

Note that the dimension of the state c in Eq. 5 coincides with the dimension of the low-dimensional basis, whereas A and $f(c)$ correspond to the projection of the spatial operator and nonlinear terms $\sigma(u)$, respectively, on the selected basis. Once Eqs. 4 and 5 are available, standard results from state estimation theory can be used to reconstruct the infinite dimensional field from a given set of measurements. However, obvious questions remain, such as how many dimensions are required for the low-dimensional description to fairly reproduce the solution and how many measurements, and at which locations, are needed to reconstruct the entire field. These questions will be addressed in the following sections.

Example: proper orthogonal decomposition of a data set

Consider a set of data $S_\ell = \{u_j\}_{j=1}^{\ell}$, obtained either by experiments or simulation. Each element of the set is an n-dimensional vector with components corresponding to the value of the field at particular locations. If several fields are involved in the description, they will be included in the vector sequentially. The set S_ℓ is assumed to be representative of the dynamic behavior of the system in the range of initial conditions, parameters, inputs, and/or perturbations of interest (Shvartsman and Kevrekidis, 1998). Given an integer k ($k \leq n$), we define the k-dimensional set $S_k = \{\phi_j\}_{j=1}^{k}$, as the *set of k orthonormal vectors* on which the average projection of the data set S_ℓ is maximized (equivalently, the k-set that minimizes the average distance to the data). Formally, the elements of this set are computed as

$$\min_{\phi_j} J(\phi_j, u)$$

$$J(\phi_j, u) = \frac{1}{\ell} \sum_{i=1}^{\ell} (u_i^T - w_i^T)(u_i - w_i) + \sum_{j=1}^{k} \lambda_j(\phi_j^T \phi_j - 1)$$

where w_i represents the projection of the data u_i on the span of the k vectors ϕ_j

$$w_i = \Phi c_i \tag{6}$$

where Φ is the matrix

$$\Phi = [\phi_1 \ \vdots \ \phi_k] \tag{7}$$

and $c_i \in R^k$ is a vector of coefficients satisfying $c_i = \Phi^T u_i$. The solution of the previous optimization problem leads to the following set of equations to be satisfied by each element in S_k

$$R\phi_j = \lambda_j \phi_j \tag{8}$$

$$R = \frac{1}{\ell} \sum_{i=1}^{\ell} u_i u_i^T \tag{9}$$

The matrix R in Eq. 9 can be considered as the discrete version of the two-point correlation function (Eq. 3) with $\mu_j = 1/\lambda_j$. In this way, any element u_i of the data set S_ℓ can be expressed in terms of S_k as

$$u_i = \Phi c_i + \varepsilon_i \tag{10}$$

where ε_i is an error vector, orthogonal to S_k, that indicates the distance at which each data point lies from the low-dimensional projection plane. The average distance of the data set to S_k is computed as

$$D_{av}^2 = \frac{1}{\ell} \sum_{i=1}^{\ell} d_i^2 = \frac{1}{\ell} \sum_{i=1}^{\ell} u_i^T u_i - \sum_{i=1}^{k} \lambda_i \tag{11}$$

Note that for $k = \ell$, $D_{av} = 0$ and we have

$$\sum_{i=1}^{\ell} \lambda_i = \frac{1}{\ell} \sum_{i=1}^{\ell} u_i^T u_i \tag{12}$$

so that the eigenvalues λ_i provide a measure of how close the data are to the set S_k. The nearer k is to ℓ, the smaller the average distance. By combining Eqs. 11 and 12 we have the equivalent expression

$$D_{av} = \left(\sum_{i=k+1}^{\ell} \lambda_i \right)^{1/2} \tag{13}$$

The selection of the dimension of the low-dimensional set is usually done by means of some related measures, known as the fraction of energy captured, or lost by the reduced order description, and defined respectively, as

$$E = \frac{\sum_{i=1}^{k} \lambda_i}{\sum_{i=1}^{\ell} \lambda_i} \tag{14}$$

$$L = 1 - E \tag{15}$$

Estimation from Measurements

Let us consider a set of k orthonormal and n-dimensional vectors $S_k = \{\phi_i\}_{i=1}^{k}$, representative of a given system (Eq. 1) in the sense described in the previous section. In addition, we define the operator $P_m \in R^{m \times n}$ as that which projects any vector $v \in R^n$ on m of its n coordinates so that $v_m = P_m v$. Then, if v_m is a vector of measurements, and v an element of the data set S_ℓ, the estimation problem consists of reconstructing the remaining $n - m$ components of v from the available measurements. A static estimate $\hat{v}$ can be produced as follows:

(1) Project Eq. 10 onto the subspace of the m coordinates defined by P_m and denoted as M_m (which we will call the *measurement subspace*), so that

$$\hat{v}_m = P_m \Phi \hat{c} + P_m \varepsilon \tag{16}$$

where $P_m \varepsilon$ is the projection of the error associated with the low-dimensional set on the subspace of measurements.

(2) Find the coefficient vector $\hat{c}$ in Eq. 16 that minimizes the distance between the data v_m and the estimates $\hat{v}_m$. This leads to the following minimum least-squares problem

$$\min_{\hat{c}} (v_m - P_m \Phi \hat{c})^T (v_m - P_m \Phi \hat{c}) \tag{17}$$

A collection of efficient numerical solution methods to solve Eq. 17 can be found in Golub and Van Loan (1983). For the present discussion, however, it is enough to know that the solution has the form

$$\hat{c} = (QQ^T)^{-1} Q v_m \tag{18}$$

with

$$Q = \Phi^T P_m^T \tag{19}$$

The estimate $\hat{v}$ of the unmeasured states is now reconstructed as

$$\hat{v} = P_m^{\perp} \Phi \hat{c} = P_m^{\perp} \Phi (QQ^T)^{-1} Q v_m \tag{20}$$

where $P_m^{\perp}$ denotes the orthogonal complement of the measurement subspace M_m.

The infinite dimensional state can also be reconstructed at a dynamic level from measurements v_m, by solving the following set of differential equations

$$\hat{c}_t = A\hat{c} + f(\hat{c}) + \Omega(v_m - Q^T \hat{c})$$

$$\hat{v} = \Phi \hat{c} \tag{21}$$

where $\hat{c}$ represents the estimates and Ω is a gain matrix that determines the (temporal) rate at which the estimate $\hat{c} \rightarrow c$. Equation 21 consists of a replica of system 5 with an extra term that, by computing the difference between the measurements and the state estimates, drives the estimated state $\hat{c}$ toward the "true" state c. The following result, adapted to nonlinear systems of the form of Eq. 5 from a standard theorem on observability properties of linear systems (Rugh, 1993), relates the rate of convergence to the minimum eigenvalue associated with the matrix QQ^T.

Theorem 1 *Let the system*

$$c_t = Ac + f(c)$$

$$v_m = Q^T c \tag{22}$$

be such that: $\|A\| = \max_{\|x\|=1} \|Ax\| = \alpha_m$, $\|f(c_1) - f(c_2)\| \leq \beta \|c_1 - c_2\|$ *and*

$$\lambda_u I \geq QQ^T \geq \lambda_l I \tag{23}$$

The observer (Eq. 21) with $\Omega = P^{-1}Q$, *and* P *being a symmetric, positive definite matrix satisfying*

$$(A + \alpha I)^T P + P(A + \alpha I) = QQ^T \tag{24}$$

with $0 < \eta < 1$ *and* $\alpha > \alpha_m + \beta \lambda_u / [(1 - \eta)\lambda_l]$, *will make the states* $\hat{c} \rightarrow c$ *at an exponential rate proportional to* $\eta \lambda_l$.

Proof: See Appendix A.

Remark 1. Note that condition A2 ensures observability of the states c in system A1, given that the observability Grammian

$$G = \int_t^{t+T} c(s)^T QQ^T c(s) ds$$

is always positive definite, provided that the number of measurements is larger than, or equal to, the dimension of the reduced order model. In this way, sensor redundancy ensures state reconstruction independently of the particular structure of the dynamical system A1. In addition, the selection of those measurements that maximize the minimum eigenvalue λ_l will guarantee fast convergence rates of observers designed according to the previous theorem.

Maximum angle between linear subspaces

As shown in the previous Theorem, the quality of the estimation is, to a large extent, conditioned by the eigenvalues of the matrix QQ^T. A geometrical interpretation of the estimation problem both at a static and dynamic level is illustrated in Figure 1 on a 3D case. There, v represents the data point to be estimated from measurements v_m located in M_m. The small circles represent the error on the estimation induced by the minimization, its radius being $r = |v_m - \hat{v}_m|$, or equivalently

$$r = (\varepsilon^T P_m^T P_m \varepsilon)^{1/2}$$

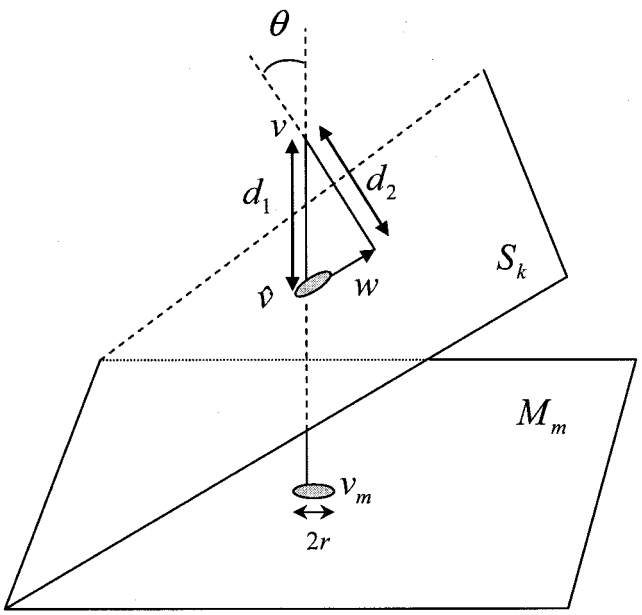

Figure 1. Relative positions of the low-dimensional subspace S_k and the space of measurements M_m.

v represents a data point lying at a distance d_2 from the low-dimensional set and v_m, its projection on the measurement subspace. The data point $\hat{v}$, reconstructed from measurements, will be on the low-dimensional set S_k at a distance d_1 ($>d_2$) from the *true* data. The smaller the angle between both subspaces, the smaller the distance d_1, thus improving reconstruction accuracy.

Note in the figure the effect that the angle between subspaces S_k and M_m has on the distance d_1 between the estimate $\hat{v}$ and the experimental data v. By construction, d_1 and d_2 are related as

$$d_1 = \frac{d_2}{\cos\theta} \tag{25}$$

where θ, in the figure, is the angle between the measurement subspace M_m and the low-dimensional set S_k. Thus, small angles (almost parallel subspaces) imply accurate estimation, at least up to the inherent error ε. Large angles, however, will cause deterioration of the accuracy of the estimation, to the point of making it completely useless in the extreme case $\theta \to \pi/2$. These considerations can be formally extended to general linear subspaces as follows:

Let us consider two linear subspaces $S_k = \{\phi_i\}_{i=1}^k$ and $S_m = \{\pi_i\}_{i=1}^m$, with elements being n-dimensional vectors and two generic unit length vectors $a = \Phi\alpha$, and $b = \Pi\beta$, lying on S_k and S_m, respectively. $\alpha \in R^k$ and $\beta \in R^m$ are coefficient vectors satisfying $\|\alpha\| = \|\beta\| = 1$, and Φ and Π matrices defined as

$$\Phi = [\phi_1, \ldots, \phi_k]$$

$$\Pi = [\pi_1, \ldots, \pi_m]$$

The angle between vectors a and b can be computed from their scalar product as

$$\cos\theta = a^T b = \alpha^T \Phi^T \Pi \beta \tag{26}$$

In addition, from the singular value decomposition theorem (Golub and Van Loan, 1996), we have orthonormal matrices U and V related as

$$U^T Q V = \Sigma \tag{27}$$

where $Q = \Phi^T\Pi$. Σ is a diagonal matrix containing as nonzero elements the singular values, σ_i, of Q. Defining u_i^T and v_i as the ith row and ith column of U and V, respectively, we have from Eq. 27 that $u_i^T Q v_i = \sigma_i$ for $i = 1, \ldots, \min(k, m)$. Comparing this expression with Eq. 26 (with u_i and v_i instead of α and β, respectively) allows us to interpret singular values in terms of angles formed by vectors in subspaces S_k and S_m, the relation being given by $\cos\theta_i = \sigma_i$. Moreover, the rows/columns of U and V constitute a basis for α and β, respectively, so that the angles between S_k and S_m are bounded as

$$\sigma_{\min} \le \cos\theta \le \sigma_{\max}$$

In our context, S_k coincides with the low-dimensional set and S_m with the (to be determined) measurement subspace M_m. Accordingly, matrix Q becomes

$$Q = \Phi^T P_m^T \tag{28}$$

From this perspective, we suggest the use of the maximum angle between subspaces as a criterion to select the appropriate measurement subspace, compatible with the constraints (number of measurements and dimension of the low-dimensional set). Thus, to improve the quality of the estimation, we choose to minimize the maximum angle between these subspaces. This is equivalent to maximizing the minimum singular value associated with matrix Q, which in turn implies maximizing the minimum eigenvalue of QQ^T in Eqs. 18 and 19 (static estimation) or in Eq. A2 (see Appendix A) for dynamic observer design. Assuming m k, the optimization problem is stated as follows

$$\max_{P_m} \min_{i=1,k} \sigma_i \tag{29}$$

Because $\sigma_i(Q) = \sqrt{\lambda_i(QQ^T)}$ (that is, the singular values of matrix Q are the square root of the eigenvalues of the matrix QQ^T), we have the following equivalent optimization problem

$$\max_{P_m} \min_{i=1,k} \lambda_i(QQ^T) \tag{30}$$

The Optimal Placement of Sensors

In this section we propose a guided search method that will approximate the solution of problems 29 and 30. Note that both equivalent problems could be solved by an exhaustive search among all possible projections P_m. Although feasible in a few number of dimensions, this solution approach is unsuitable for most cases of practical interest. Alternatively, by taking advantage of the underlying structure of Q, we propose a systematic algorithm to approximate the solution. Before the algorithm is formally described, we illustrate its main features on a simple three-dimensional example.

Motivating example

Consider a set S_2 of the form

$$\Phi = \begin{bmatrix} 0.5141 & 0.0490 \\ 0.5011 & -0.8274 \\ 0.6961 & 0.5595 \end{bmatrix} \tag{31}$$

The problem consists of selecting the best two measurements from the three possible locations (rows in matrix Φ). For this case, there are three possible subspaces M_2, with the following projections

$$P_2^I = \begin{bmatrix} 1 & 0 \\ 0 & 1 \\ 0 & 0 \end{bmatrix}^T \qquad P_2^{II} = \begin{bmatrix} 1 & 0 \\ 0 & 0 \\ 0 & 1 \end{bmatrix}^T \qquad P_2^{III} = \begin{bmatrix} 0 & 0 \\ 1 & 0 \\ 0 & 1 \end{bmatrix}^T \tag{32}$$

In low-dimensional spaces, problem 29 or 30 can be solved in a straightforward manner by exhaustive enumeration, that is, constructing all possible combinations $\Phi^T P_2^j$, for $j = 1$, 2, and 3, and examining the eigenvalues of the corresponding $Q^T Q$ products (equivalently, the singular values of matrices Q, which, as shown in the previous section, are related to the angles between subspaces). For this particular case we have

$$(QQ^T)^I = \begin{bmatrix} 0.5154 & -0.3894 \\ -0.3894 & 0.6870 \end{bmatrix}$$

$$(QQ^T)^{II} = \begin{bmatrix} 0.7489 & 0.4187 \\ 0.4147 & 0.3154 \end{bmatrix}$$

$$(QQ^T)^{III} = \begin{bmatrix} 0.7357 & -0.0251 \\ -0.0251 & 0.9976 \end{bmatrix}$$

The minimum eigenvalue for each measurement set is, respectively, 0.2024, 0.0643, and 0.7333. From these calculations, it follows that according to the maximum angle criterion, option *III* is the optimal one because it maximizes the minimum eigenvalue. From the relationships between angles, singular values, and eigenvalues, we find the maximum angle to be

$$\cos \theta_{III} = \sqrt{\lambda_i(QQ^T)} = 0.8563$$

The improvement obtained in the quality of the estimation can be computed from Eq. 25 as follows:

If a and b are two possible choices of sensor placement with maximal angles θ_a and θ_b, respectively, the distances in the worst scenarios (maximal angles) would be related as

$$\frac{d_a}{d_b} = \frac{\cos \theta_b}{\cos \theta_a}$$

In our example, the uncertainties in the estimation between the optimal and worst options (*III* and *II*, respectively) in their worst scenarios can be related as

$$\frac{d_{III}}{d_{II}} = \frac{\sqrt{0.0643}}{\sqrt{0.7333}} = 0.2961$$

which implies a potential reduction of the estimation uncertainty of more than 70% with respect to placement *II*. As pointed out earlier, such an exhaustive search is not suitable for high dimensional spaces. In these situations, an alternative numerical method is proposed that takes advantage of the algebraic structure implicit in Eq. 28. The algorithm is based on the following observations:

(1) *In Eq. 28, the effect of P_m^T on Φ^T is that of deleting elements of the basis vectors ϕ_i at the positions where the columns of P_m are zero*. In the example considered, the optimal placement P_2^{III} deletes the first components of ϕ_1 and ϕ_2 to produce a Q matrix of the form

$$Q = \begin{bmatrix} 0.5141 & 0.5011 & 0.6961 \\ 0.0490 & -0.8274 & 0.5595 \end{bmatrix} \begin{bmatrix} 0 & 0 \\ 1 & 0 \\ 0 & 1 \end{bmatrix} = \begin{bmatrix} 0.5011 & 0.6961 \\ -0.8274 & 0.5595 \end{bmatrix}$$

(2) *The scalar products of the resulting subvectors $P_m\phi_i$ are the diagonal elements of QQ^T*. In our case, the diagonal elements in the matrix QQ^T become

$$QQ^T = \begin{bmatrix} 0.5011^2 + 0.6961^2 & \cdots \\ \cdots & 0.8274^2 + 0.5595^2 \end{bmatrix}$$

The eigenvalues of matrix QQ^T are located inside circles centered at the positions given by the diagonal elements [Gershgorin disk theorem (Golub and Van Loan, 1996)] with radii satisfying

$$r_i = \sum_{j \neq i}^{n} |(QQ^T)_{ij}| \tag{33}$$

(3) *When the radii are much smaller than the diagonal elements (denoted as s_i), problem 30 approximates that of maximizing the minimum diagonal element.* Formally, this is written for our example as

$$\max_{P_m} \min(s_1, s_2) \tag{34}$$

This assertion is trivially satisfied when the dimension of the space of measurements equals the dimension of the elements of the basis because, by orthonormality, the off-diagonal elements are zero. Of course, in this case, all eigenvalues are centered at position 1. However, as the number of measurements decreases, the resulting subvectors $P_m\phi_i$ will no longer be orthonormal, which translates into nonzero off-diagonal elements in QQ^T. In this context, the solution of problem 34 can be interpreted as *seeking for the "nearest to" orthonormal set of m-dimensional subvectors $P_m\phi_i$*. Moreover, as it will be shown in the next section, condition 3 can be quite possibly justified whenever the locations are such that $s_i \approx s_j$ for all possible i, j basis elements. Next we use the previous example to give an outline of the proposed guided search algorithm. A formal and general description is left for the next section.

To find the operator P_2 that maximizes the minimum diag-

onal element of QQ^T, we first compute for each ϕ_i a vector σ_i with elements being the square of the elements in ϕ_i; that is, $\sigma_i = [(\phi_i)_1^2, \ldots, (\phi_i)_j^2, \ldots, (\phi_i)_n^2]^T$. In our example these vectors are

$$\sigma_1 = (0.2643 \quad 0.2511 \quad 0.4846)$$

$$\sigma_2 = (0.0024 \quad 0.6846 \quad 0.3130)$$

The elements of these vectors are now sorted in decreasing order so that for σ_1 and σ_2 we have, respectively,

$$(0.4846 \quad 0.2643 \quad 0.2511) \qquad Index\ \eta_1^{(1)} = (3 \quad 1 \quad 2)$$

$$(0.6846 \quad 0.3130 \quad 0.0024) \qquad Index\ \eta_2^{(1)} = (2 \quad 3 \quad 1)$$

where the vectors $\eta_1^{(1)}$ and $\eta_2^{(1)}$ are used to store the original indexes (sensor locations) of the elements. With these preliminaries, search now proceeds by iteratively constructing sequences $\{\eta_i^{(k)}\}$ for each basis element i so that the m-summations $s_i^{(k)}$ of the elements in σ_i are nonincreasing; that is, $s_i^{(k+1)} \leq s_i^{(k)}$ for every k. In our example, $m = 2$ and the nonincreasing sequence for the first basis element is

$$s_1^{(1)}(=0.4846 + 0.2643) = 0.7489 \qquad Index\ \eta_1^{(1)} = (3 \quad 1 \quad 2)$$

$$s_1^{(2)}(=0.4846 + 0.2511) = 0.7357 \qquad Index\ \eta_1^{(2)} = (3 \quad 2 \quad 1)$$

$$s_1^{(3)}(=0.2643 + 0.2511) = 0.5154 \qquad Index\ \eta_1^{(3)} = (1 \quad 2 \quad 3)$$

The same procedure is repeated for the second basis element, thus resulting in a sequence $\{\eta_2^{(k)}\}$ for $k = 1$, 2, and 3. Figure 2 shows all possible placements for this example on the space of $m = 2$ summations $\Sigma = (s_1, s_2)$ for each basis element. The corresponding index vectors associated with each possible sensor locations are also indicated along the summation axes. At iteration 1, we compute $\eta_1^{(1)}$ and $\eta_2^{(1)}$, their corresponding summations $\Sigma_1^{(1)}$ and $\Sigma_2^{(1)}$ (see Figure 2) and the value

$$L^{(1)} = \max[\min(\Sigma_1^{(1)}), \min(\Sigma_2^{(1)})]$$

which in this case is $L^{(1)} = 0.7357$ and corresponds to locations $\Sigma_2^{(1)}$. This value is an approximation to the solution of problem 34 and will be used in the next iteration to select only those sequence elements that satisfy $L^{(2)} \geq L^{(1)}$. The procedure is then repeated until no sequence element exists that improves the previous best max–min value. This is illustrated in Figure 2, where after the first iteration, $\eta_1^{(2)}$ is the only sequence element that could improve $L^{(1)}$, and in fact coincides with the best previous value at point $\Sigma_2^{(1)}$. Therefore, this is the solution to the problem that coincides with that resulting from an exhaustive search.

Algorithm to select the optimal placement

Before proceeding with the formal description of the algorithm we note that, as pointed out in the previous section, problem 30 reduces to the much simpler statement

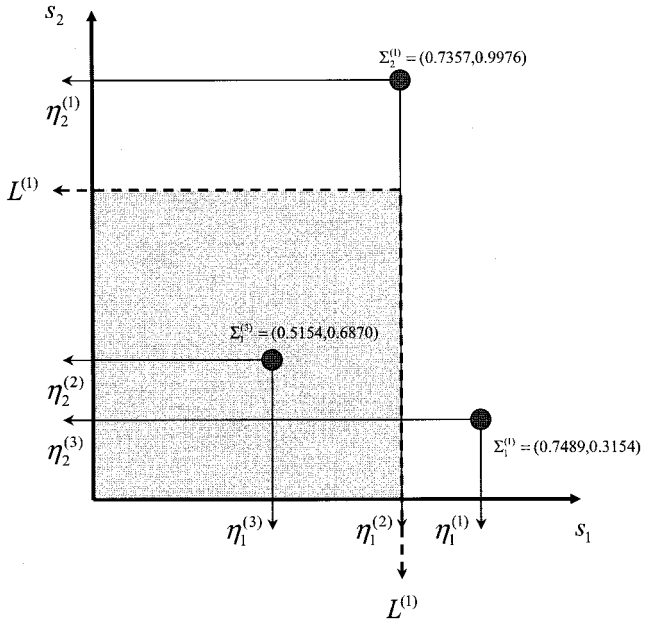

Figure 2. Structure of the search space for Example 1.

Dots indicate all possible solutions. The shadowed rectangle indicates the region where solutions better than $L^{(1)}$ cannot be found. This bound reduces the number of sequence elements to be computed in the next iteration.

$$\max_{P_m} \min(s_1, \ldots, s_k) \tag{35}$$

whenever condition 3 applies. $s_1, \ldots, s_k$ in Eq. 35 correspond with the diagonal elements of the matrix $QQ^T = \Phi^T P_m^T P_m \Phi$, of the form

$$s_1 = \sum_{j=1}^{m} (\phi_{1j})^2$$
$$\vdots$$
$$s_k = \sum_{j=1}^{m} (\phi_{kj})^2$$

The relationship between Eq. 30 and Eq. 35 holds not only as m approaches n, but also for a given m, as long as $s_i \approx s_j$ for all possible i, j elements of the basis set. This can be shown by noting that for a given P_m, each off-diagonal element $(QQ_T)_{ij}$ can be expressed as

$$\sum_{k=1}^{m} (\phi_{ik}\phi_{jk}) = \cos\theta_{ij}\sqrt{s_i s_j}$$

where θ_{ij} is the angle formed between subvectors ϕ_i^m and ϕ_j^m, with $\phi_i^m = (\phi_{i1}, \ldots, \phi_{im})$. From this expression, the following bound on $|\cos\theta_{ij}|$ can be obtained

$$|\cos\theta_{ij}| \leq \frac{\left|\sum_{k=1}^{m} (\phi_{ik}\phi_{jk})\right|}{\sqrt{s_i s_j}} \leq \frac{C}{\sqrt{s_i s_j}} \tag{36}$$

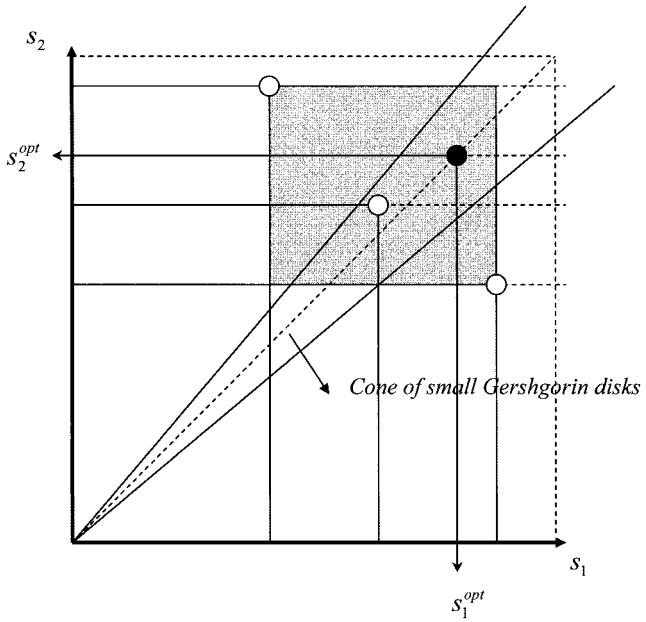

Figure 3. The search space for optimal placement.

Circles denote possible sensor configurations in the updated feasible region (shadowed rectangle). The cone sector bounding the diagonal indicates the region of small Gershgorim disks. If a solution $[s_1^{opt}, s_2^{opt}]$ exists in this region, this solution will be the optimal one for both problems 30 and 35.

where the righthand side of this inequality is a function that achieves its minimum value for $s_i = s_j$. Thus solutions P_m of Eq. 35, which in addition lead to $s_i \approx s_j$ for all possible i, j ensure that the radii of the corresponding Gershgorin disks will be small, thus allowing problem 35 to be a good approximation of problem 29 or 30. This situation is represented in Figure 3.

Algorithm description

For each element $\phi_i \in R^n$ of the set S_k, let us consider the vectors $\sigma_i = [(\phi_i)_1^2, \ldots, (\phi_i)_j^2, \ldots, (\phi_i)_n^2]^T$, $I_i = [1:n]$ (see Appendix B for notation summary) and an index vector $\eta_i \in Z^m$ with elements being elements of I_i. In addition, we define the operator $\Im(\sigma_i, \eta)$ as that which computes the summation of elements in σ_i with indexes $[(\eta)_1, \ldots, (\eta)_m]^T$. Using standard compact notation this is written as

$$\Im(\sigma_i, \eta) = sum[\sigma_i(\eta_i)]$$

$$s_i = \Im(\sigma_i, \eta)$$

For a given sequence of index vectors $\{\eta^{(p)}\}$ we also have

$$\Im(\sigma_i, \{\eta^{(p)}\}) = \{\Im(\sigma_i, \eta^{(p)})\} = \{s_i^{(p)}\}$$

A point Σ in the k-summation space is obtained as

$$\Sigma(\eta, S_k) = [\Im(\sigma_1, \eta), \ldots, \Im(\sigma_k, \eta)]$$

$$\Sigma(\eta, S_k) = [s_1, \ldots, s_k] \tag{37}$$

In the same way, a sequence of points is obtained by applying Eq. 37 to a sequence $\{\eta^{(p)}\}$ so that

$$\Sigma(\{\eta^{(p)}\}, S_k) = [\Im(\sigma_1, \{\eta^{(p)}\}), \ldots, \Im(\sigma_k, \{\eta^{(p)}\})]$$

$$\Sigma(\{\eta^{(p)}\}, S_k) = \{\Sigma(\eta^{(p)}, S_k)\} = \{\Sigma^{(p)}\}$$

A nonincreasing sequence of r index vectors $\{\eta_i^{(p)}\}$ is defined as that which satisfies

$$\Im(\sigma_i, \eta_i^{(p)}) \le \Im(\sigma_i, \eta_i^{(p-1)})$$

for $p = 2, \ldots, r$.

Conditional sequences $\{\eta_i^{(p)}\}_{[a,b,c]}$ are defined as nonincreasing sequences which for every $p = 1, \ldots, r$ satisfy

$$\sup(a, c) \le \Im(\sigma_i, \eta_i^{(p)}) \le b \tag{38}$$

$$c \le \Im(\sigma_j, \eta_i^{(p)}) \qquad \text{for } j = 1, \ldots, k; j \ne i \tag{39}$$

If either Eq. 38 or Eq. 39 does not hold for every $p = 1, \ldots, r$, the sequence is empty; that is, $\{\eta_i^{(p)}\}_{[a,b,c]} = \varnothing$. A conditional sequence $\{\eta_i^{(p)}\}_{[a,b,c]}$ is *incomplete* if there exists some $c \notin \{\eta_i^{(p)}\}_{[a,b,c]}$ satisfying either Eq. 38 or Eq. 39. If not, the conditional sequence is *complete*. A method to compute complete conditional sequences is presented in Appendix B. Using these definitions, the algorithm is summarized as follows:

Initialization

Set up positive numbers a, $L^{(0)}$, and $\{\bar{L}_i\}$ for every $i = 1, \ldots, k$ as $\bar{L}_i = \max_{\eta_i} \Im(\sigma_i, \eta_i)$.

Iteration step (from $\ell = 0$)

1. For a given integer ℓ, set up positive numbers $L^{(\ell)}$ and define for each i, intervals $[\underline{L}_i, \bar{L}_i]$ with $\underline{L}_i = \bar{L}_i - \varepsilon$
2. For each $i = 1, \ldots, k$
3. Compute the complete conditional sequence $\{\eta_i^{(p)}\}_{[\underline{L}_i, \bar{L}_i, L^{(\ell)}]}$ (see Appendix B) and its corresponding sequence of points $\{\Sigma^{(p)}\}_{[\underline{L}_i, \bar{L}_i, L^{(\ell)}]}$
4. Compute $L_i = \max_p\{\min[\Sigma_1^{(p)}], \ldots, \min[\Sigma_k^{(p)}]\}_{[\underline{L}_i, \bar{L}_i, L^{(\ell)}]}$
5. If L_i $L^{(\ell)}$ store current p, set up $L^{(\ell)} = L_i$, and go to step 2 for the next i up to k
6. If $L^{(\ell)} \ge \bar{L}_j$ for some $j = 1, \ldots, k$, stop along j
7. If step 6 holds for every $j = 1, \ldots, k$, save solution p, $\eta_i^{(p)}$ and terminate. If not, set $L^{(\ell+1)} = L^{(\ell)}$, $\bar{L}_i = \underline{L}_i$ for every $i \ne j$, and go to step 1 with $\ell = \ell + 1$

Remark 2. Note that an alternative, although suboptimal, approach to problem 35 can be produced by selecting for each $j = 1, \ldots, m$ the location that maximizes the minimum summation $(s_1, \ldots, s_k)$ (see Alvarez et al., 1981). The algorithm steps can be summarized as follows:

1. Set up $j = 1$, $\eta = [\,]$, $K = [1:n]$
2. Find some $k \in K$ such that

$$\max_{k} \min_{i} [\Im(\sigma_i, k)] \tag{40}$$

3. Store k in η so that $\eta = [\eta, k]$
4. Set $K = K/k$ (that is, delete k from K), $j = j + 1$, and go to step 5
5. If $j = m$ stop; otherwise, go to step 2

This approach, which we will call *sequential*, will be compared in the next section with the one we have presented here.

Case Studies

In this section, the different features of the proposed technique are illustrated on two case studies involving diffusion and diffusion–reaction processes. The first example concentrates on the algorithmic aspects of determining sensor placement, whereas the second example will serve to explore the effects of sensor placement on the performance of the dynamic observer (Eq. 21) for field reconstruction.

Diffusion process

Let us consider the set $S_k = \{\phi_i\}_{i=1}^{2}$ as the one defining a two-dimensional subspace that captures the most relevant dynamic features of a given diffusion process. Note that, although larger dimensional subspaces are usually required to provide a fairly accurate description of this type of processes, the two-dimensional structure is preserved here for illustration purposes. In this example, the elements ϕ_i correspond with the eigenfunctions of the one-dimensional Laplace operator, satisfying the following equation

$$\Delta\phi = -\lambda\phi$$

on the one-dimensional compact domain $x \in (0, 1)$ with boundary conditions

$$\phi(0) = \phi(1) = 0$$

The solution of this problem results in a set of eigenfunctions of the form

$$\phi_i(x) = \sqrt{2}\,\sin(\pi i x) \qquad \text{for } i = 1, \ldots, \infty \tag{41}$$

A plot of the first two eigenfunctions in presented in Figure 4. The algorithm described in the previous section is used to determine, according to criterion 35, the best possible measurement locations for sensors sets ranging between 5 and 15, on a discretization basis of 32 points. The intermediate points Σ attained by the search algorithm in the 2-summation space, and the corresponding minimum and maximum eigenvalues of the QQ^T matrix, are presented in Figure 5. Note that as search proceeds and the diagonal elements become closer, points are reached (and thus sensor arrangements) with nearby eigenvalues that correspond to "nearest to" orthonormal set of m-dimensional subvectors $P_m\phi_i$, as discussed earlier. The spatial placement of sensors producing such subvectors are depicted in Figure 6 for different sets of available measurements.

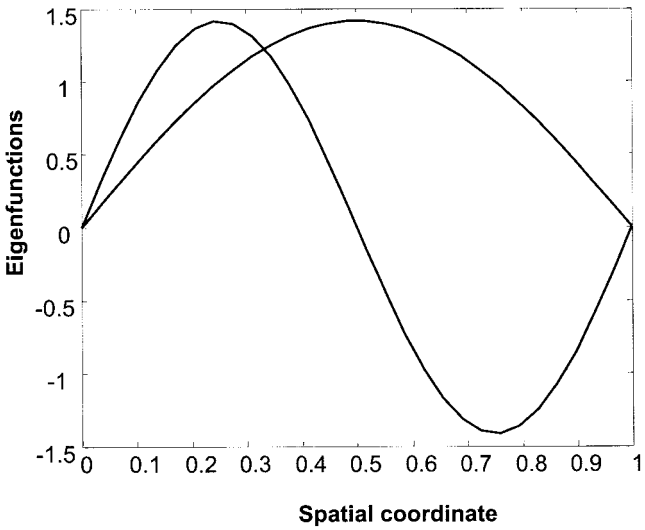

Figure 4. The first two eigenfunctions (ϕ_1, ϕ_2) for the diffusion example as a function of the position.

A Nonlinear Convection–Diffusion–Reaction Process

In this example we consider the problem of concentration and temperature reconstruction on a nonisothermal tubular reactor from a limited number of sensors. The system is described by the following set of partial differential equations (Antoniades and Christofides, 2001b) defined on a spatial domain $z \in (0, 1)$

$$C_t = -\frac{\partial C}{\partial z} + \frac{1}{\mathrm{Pe}_C}\frac{\partial^2 C}{\partial z^2} - f(C, T) \tag{42}$$

$$T_t = -\frac{\partial T}{\partial z} + \frac{1}{\mathrm{Pe}_T}\frac{\partial^2 T}{\partial z^2} + B_T f(C, T) + \beta_T(T_c - T) \tag{43}$$

where C and T stand for concentration and temperature, respectively, in deviation form with respect to a stationary state. T_c corresponds to the temperature of the cooling medium and $f(C, T)$ represents the reaction term, of the form

$$f(C, T) = B_C(1 + C)\exp\left(\frac{\gamma T}{1 + T}\right)$$

The parameters used in the simulation are taken from Antoniades and Christofides (2001b), with values

$$\mathrm{Pe}_C = 7.0 \qquad B_C = 0.1 \qquad \gamma = 10.0$$

$$\mathrm{Pe}_T = 7.0 \qquad B_T = 2.5 \qquad \beta_T = 2.0$$

The reactant at the output stream is assumed to be recycled to the feed stream at a ratio r, which results into the following boundary conditions at $z = 0$

$$\frac{\partial C}{\partial z} = \mathrm{Pe}_C[(1 - r)C_0 + rC(t, 1) - C(t, 0)]$$

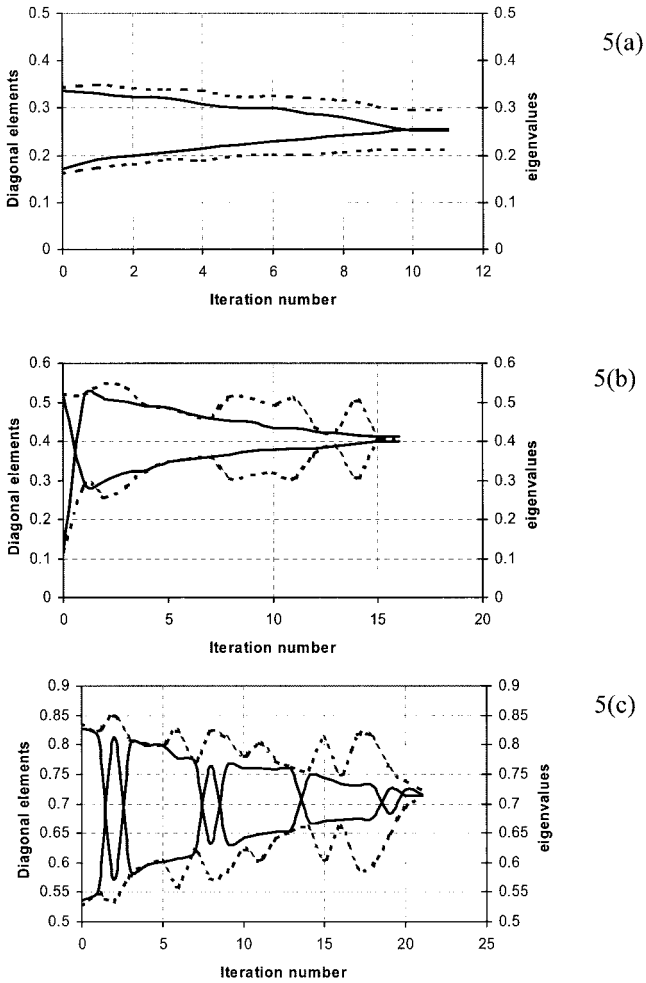

Figure 5. Intermediate points (diagonal elements) in the *k*-summation space (solid lines) and the corresponding maximum and minimum QQ^T eigenvalues (dotted lines) for the diffusion example as a function of the iteration number for different numbers of sensors.

(a) $m = 5$; (b) $m = 8$; (c) $m = 15$.

$$\frac{\partial T}{\partial z} = \mathrm{Pe}_T[(1 - r)T_0 + rT(t, 1) - T(t, 0)]$$

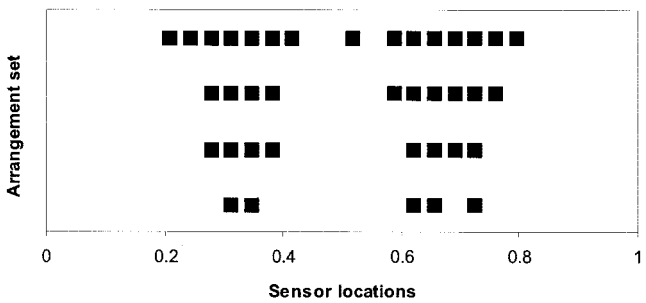

Figure 6. Optimal sensor arrangements for different number of available sensors.

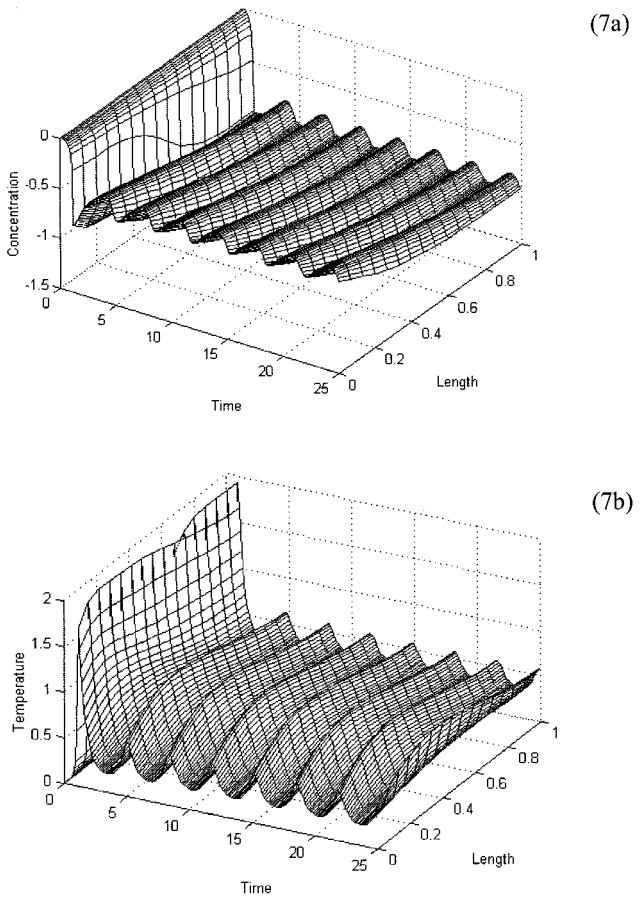

Figure 7. Snapshots produced by direct numerical simulation of the nonlinear diffusion–convection reaction system (Eqs. 42 and 43).

(a) Concentration evolution; (b) temperature evolution.

The corresponding boundary conditions at $z = 1$ are

$$\frac{\partial C}{\partial z} = \frac{\partial T}{\partial z} = 0$$

Operating at $C_0 = T_0 = T_c = 0$ with a recycling relation $r = 0.5$, the reactor exhibits oscillations as illustrated in Figure 7. The set S_k is constructed as the POD basis associated with the discrete version of the two-point correlation kernel (Eq. 3), described earlier in section 2 (see also Holmes et al., 1996). The snapshots used are depicted in Figures 7a and 7b for C and T, respectively. Each snapshot consists of the values of concentration and temperature at a given time taken at 16 equally spaced positions in the domain, and ordered sequentially in a vector $u = (C^T, T^T)^T$. The energy captured by the first 11 modes (Eq. 14) is plotted in Figure 8, showing that three POD basis functions are enough to collect more than the 99.9% of the energy (Eq. 14), thus capturing most of the relevant dynamic features of the system. The selected POD basis is depicted in Figure 9a for concentration and Figure 9b for temperature.

For the selected basis set and different numbers of possible given measurements (m values of 6, 8, 10), sensor placements satisfying Eq. 35 were computed with the algo-

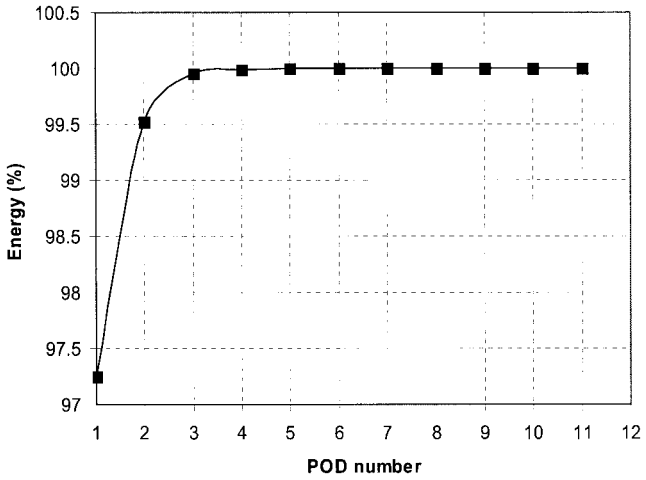

Figure 8. Energy captured by the low-dimensional set as a function of the number of PODs chosen.

Note that three PODs are enough to capture more than 99.9% of the energy of the system.

rithm described earlier in section 4. Figure 10 represents, for the different number of sensors available, both the values of the diagonal elements of matrix QQ^T and their correspond-

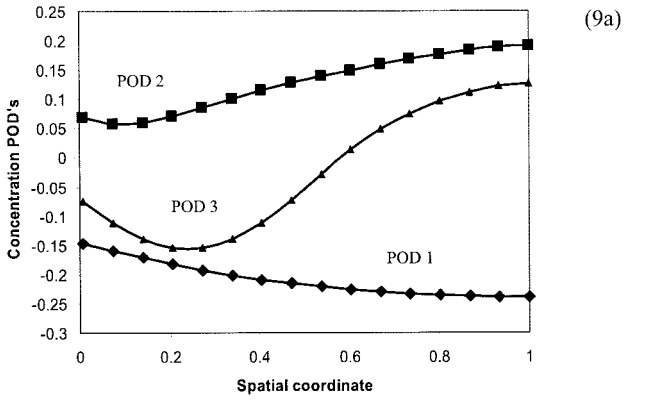

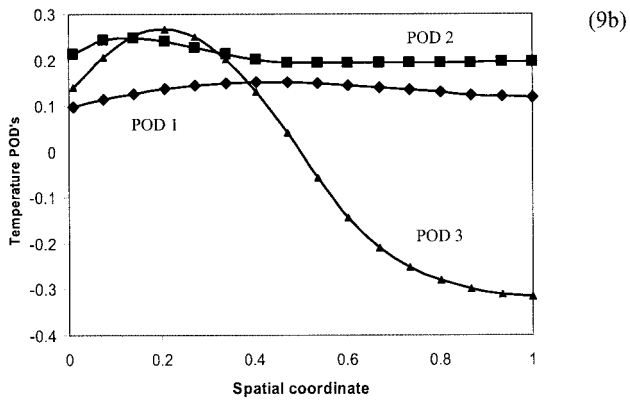

Figure 9. The first three PODs functions chosen in accordance with the energy criterion.

(a) Concentration part of the discretized PODs functions. (b) Temperature part of the discretized PODs functions.

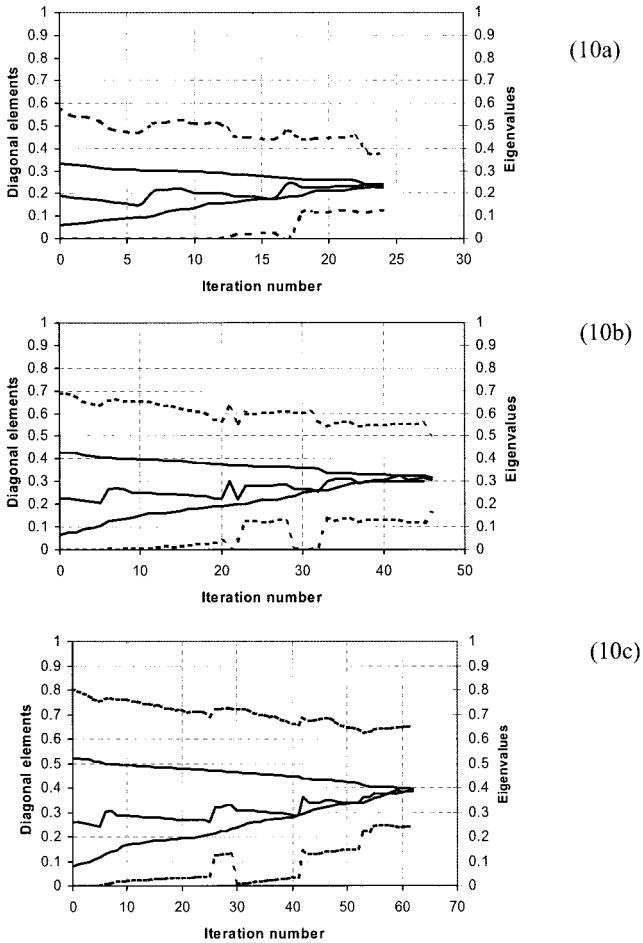

Figure 10. Intermediate points (diagonal elements) in the *k*-summation space (solid lines) and the corresponding maximum and minimum QQ^T eigenvalues (dotted lines) for the nonlinear convection–diffusion–reaction example, as a function of the iteration number for different numbers of sensors.

(a) $m = 6$; (b) $m = 8$; (c) $m = 10$.

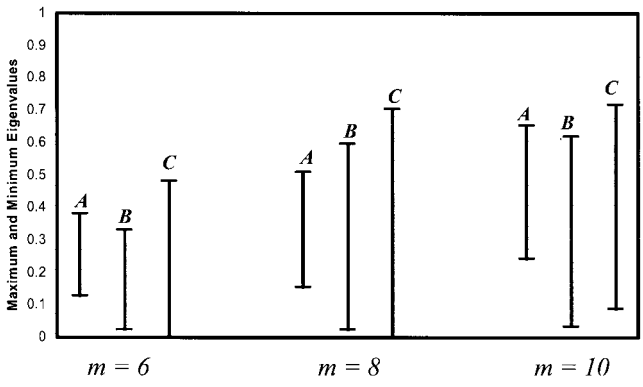

Figure 11. A comparison of the maximum and minimum QQ^T eigenvalues, for different number of sensors, obtained by (A) optimal solution of problem 35, (B) sequential approach as suggested in Remark 1, and (C) maximization of the trace of QQ^T.

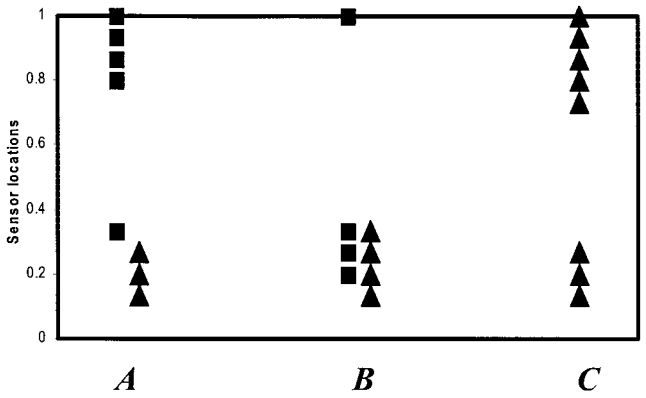

Figure 12. Optimal sensor arrangements for $m = 8$ attained by methods A, B, and C, respectively.

Squares indicate the location of temperature sensors. Triangles indicate the location of concentration sensors.

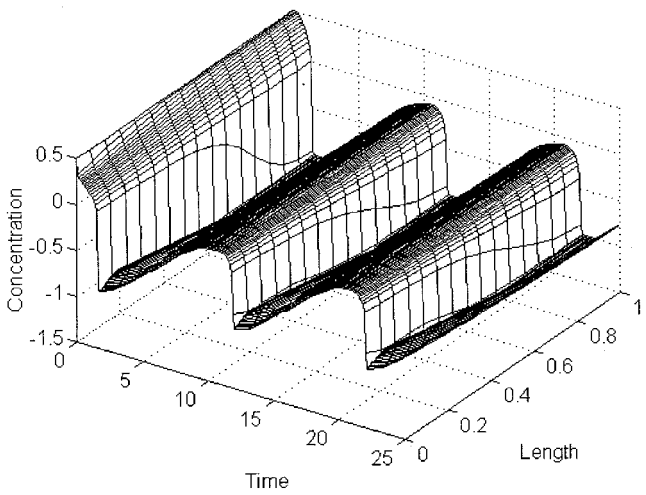

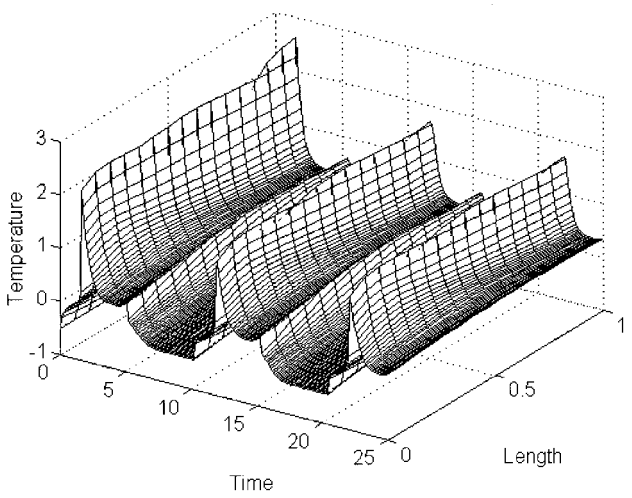

Figure 13. Concentration and temperature evolution profiles for the nonisothermal chemical reactor in response to temperature fluctuations in the fresh reactant feedstream (the range and shape of the fluctuation are depicted in Figures 14 and 15, respectively).

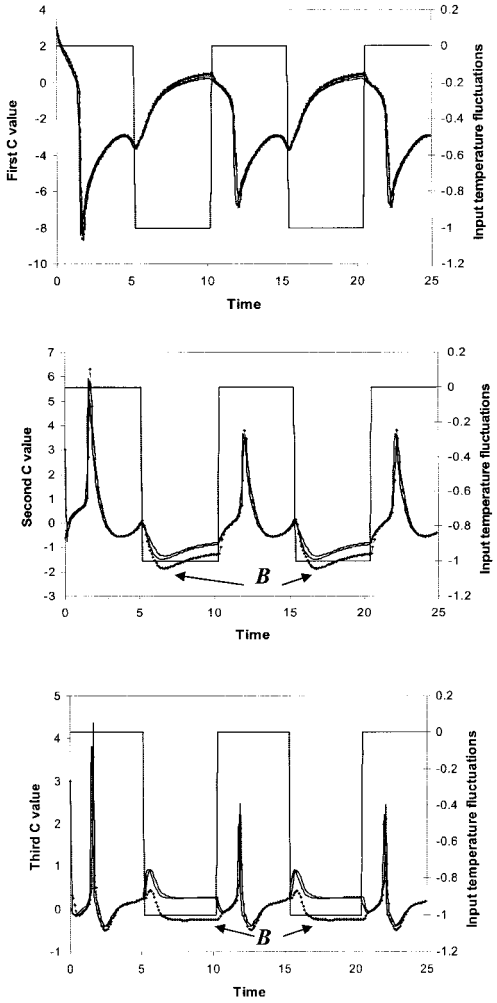

Figure 14. Evolution of the real and the estimated first three modes under temperature input fluctuation and eight available sensors.

Mode estimation is obtained from the observation scheme (Eq. 21) with gain computed as in Theorem 1. Solid lines represent the evolution of the real modes and modes estimated from sensor arrangements (A). Dotted lines represent the evolution of modes for sensor arrangement (B).

ing minimum and maximum eigenvalues obtained as a function of the iteration number. The arrangements obtained (presented in Figure 12) are compared in Figure 11, in terms of the maximum and minimum eigenvalues of the resulting QQ^T matrix, with other selection techniques suggested in the literature (see Alvarez et al., 1981). Two techniques were considered: on the one hand, a sequential approach to problem 35 described as a remark at the end of section 4 (Eq. 40) and represented in Figure 11 as **B**. On the other hand, a selection procedure based on the maximization of the trace is associated with matrix QQ^T and denoted by **C**. As may be seen in the figure, the approach suggested herein is able to identify sensor arrangements with minimum eigenvalues much larger than those obtained through procedures **B** and **C**. In accordance with the discussion in section 3, this would imply better estimation properties both at the static and the dynamic levels. To confirm this fact, observation experi-

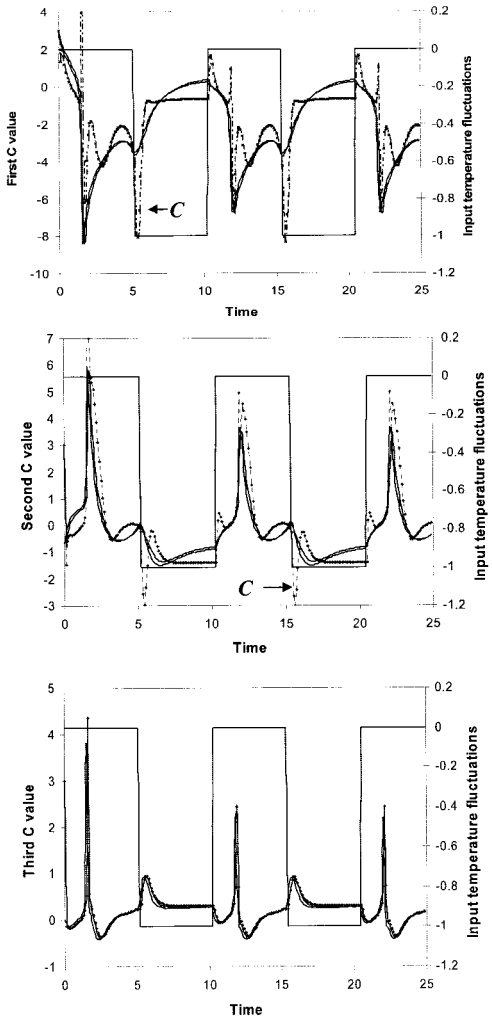

Figure 15. Evolution of the real and the estimated first three modes under temperature input fluctuation and eight available sensors.

Mode estimation is obtained from the observation scheme (Eq. 21) with gain computed as in Theorem 1. Solid lines represent the evolution of the real modes and modes estimated from sensor arrangements (A). Dotted lines represent the evolution of modes for sensor arrangement (C).

ments were carried out with these three possible arrangements. The system, in these experiments, was perturbed by a fluctuation in the fresh feed stream temperature. The distribution of temperature and concentration under such perturbation is plotted in Figure 13 (the class of perturbation introduced in the system is represented in Figures 14 and 15). The evolution of the first (dominant) *true c*-states and the ones estimated with the proposed observation scheme (Eq. 21), but different arrangements, are presented in Figures 14 and 15. As illustrated there, the ability to dynamically observe the dominant modes of the system is to a large extent conditioned by the type of sensor arrangement. In this way, the criterion proposed herein induces a very acceptable observer performance as compared with the alternative selection criteria (especially the criterion based on maximizing the trace).

Conclusions

In this communication we presented a systematic technique to solve the sensor placement problem by taking advantage of the time scale separation properties of dissipative systems (leading to low-dimensional long term dynamics) as well as notions related to the angle between subspaces.

First, a low-dimensional representation of the solution associated with the original distributed system is obtained. Then, sensors are chosen so that the measurement subspace has the largest possible minimum angle with respect to the low-dimensional subspace where the state resides. A guided search algorithm was proposed to this purpose. The resulting sensor configuration was seen to be advantageous in reconstructing the field from a limited number of available measurements. The main ingredients of this methodology were illustrated on relevant examples involving diffusion and nonlinear diffusion–convection–reaction processes.

Acknowledgments

A.A.A. acknowledges the generous support from Xunta de Galicia and Universidade de Vigo; I.G.K. acknowledges support from the National Science Foundation and the AFOSR (Dynamics and Control Program, Dr. Marc Jacobs).

Literature Cited

Alvarez, J., J. A. Romagnoli, and G. Stephanopoulos, "Variable Measurements Structures for the Control of a Tubular Reactor," *Chem. Eng. Sci.*, **36**(10), 1695 (1981).

Antoniades, C., and P. D. Christofides, "Integrating Nonlinear Output Feedback Control and Optimal Actuator/Sensor Placement for Transport-Reaction Processes," *Chem. Eng. Sci.*, **56**, 4517 (2001a).

Antoniades, C., and P. D. Christofides, "Studies on Nonlinear Dynamics and Control of a Tubular Reactor with Recycle. Nonlinear Analysis," *Theor. Methods & Appl.*, **47**, 5933 (2001b).

Courant, R., and D. Hilbert, *Methods of Mathematical Physics*, Wiley, New York (1937).

Golub, G. H., and C. Van Loan, *Matrix Computations*, Johns Hopkins University Press, Baltimore, MD (1983).

Harris, T. J., J. D. Wright, and J. F. MacGregor, "Optimal Sensor Location with an Application to a Packed Bed Tubular Reactor," *AIChE J.*, **26**(6), 910 (1980).

Holmes, P., J. L. Lumley, and G. Berkooz, *Turbulence, Coherent Structures, Dynamical Systems and Symmetry*, Cambridge University Press, Cambridge, UK (1998).

Kammer, D. C., "Optimal Sensor Placement for Model Identification Using System Realization Methods," *J. Guidance & Control*, **19**(3), 729 (1991).

Keller, J. P., and D. Bonvin, "Selection of Input and Output Variables as a Model Reduction Problem," *Automatica*, **28**(1), 171 (1992).

Khalil, H. K., *Nonlinear Systems*, Prentice Hall, Upper Saddle River, NJ (1996).

Kubrusly, C. S., and H. Malebranche, "Sensors and Controllers Location in Distributed Systems—A Survey," *Automatica*, **21**, 117 (1985).

Kumar, S., and J. H. Seinfeld, "Optimal Location of Measurements for Distributed Parameter Estimation," *IEEE Trans. Autom. Control.*, **AC23**(4), 690 (1978).

Podvin, B., and J. Lumley, "Reconstructing the Flow in the Wall Region from Wall Sensors," *Physics of Fluids*, **10**(5), 1182 (1998).

Raich, A., and A. Cinar, "Diagnosis of Process Disturbances by Statistical Distances and Angle Measures," *Comp. Chem. Eng.*, **21**(6), 661 (1997).

Rugh, W. J., *Linear System Theory*, Prentice Hall, Englewood Cliffs, NJ (1993).

Shvartsman, S. Y., and I. O. Kevrekidis, "Nonlinear Model Reduction for Control of Distributed Systems: A Computer-Assisted Study," *AIChE J.*, **44**(7), 1579 (1998).

Van der Berg, F. W. J., H. C. J. Hoefsloot, H. F. M. Boelens, and A. K. Smilde, "Selection of Optimal Sensor Position in Tubular Reactor Using

Robust Degree of Observability Criteria," *Chem. Eng. Sci.*, **55**, 827 (2000).
Vande Wouwer, A., N. Point, S. Porteman, and M. Remy, "An Approach to the Selection of Optimal Sensor Locations in Distributed Parameter Systems," *J. Proc. Control*, **10**, 291 (2000).
Windes, L. C., A. Cinar, and W. H. Ray, "Dynamic Estimation of Temperature and Concentration Profiles in Packed Bed Reactors," *Chem. Eng. Sci.*, **44**(10), 2087 (1989).

Appendix A

Theorem 2 *Let the system*

$$c_t = Ac + f(c)$$

$$v_m = Q^T c \tag{A1}$$

be such that: $\|A\| = \max_{\|x\|=1}\|Ax\| = \alpha_m$, $\|f(c_1) - f(c_2)\| \le \beta\|c_1 - c_2\|$ *and*

$$\lambda_u I \ge QQ^T \ge \lambda_l I \tag{A2}$$

The observer (Eq. 21) with $\Omega = P^{-1}Q$, *and* P *being a symmetric, positive definite matrix satisfying*

$$(A + \alpha I)^T P + P(A + \alpha I) = QQ^T \tag{A3}$$

with $0 < \eta < 1$ *and* $\alpha > \alpha_m + \beta\lambda_u/[(1 - \eta)\lambda_l]$, *will make the states* $\hat{c} \to c$ *at an exponential rate proportional to* $\eta\lambda_l$.

Proof: First, note that the error between the estimates and the states $\varepsilon = c - \hat{c}$ evolves in time as

$$\varepsilon_t = (A - P^{-1}QQ^T)\varepsilon + f(c) - f(\hat{c})$$

The proof is made in the following steps:

1. Construct a symmetric matrix P as

$$P = \int_0^\infty e^{-(A+\alpha I)^T t} QQ^T e^{-(A+\alpha I)t} dt$$

The matrix P is positive definite, given that QQ^T satisfies Eq. A2. It is also bounded because the differential system $y_t = -(A + \alpha I)y$ is exponentially stable for any $\alpha > \alpha_m$. In fact, given an arbitrary vector y_0, the quadratic form $y_0^T P y_0$ is bounded as

$$y_0^T P y_0 \le \frac{\lambda_u}{2(\alpha - \alpha_m)} y_0^T y_0$$

By construction, P also satisfies Eq. A3: Let $H(t) = e^{-(A+\alpha I)^T t} QQ^T e^{-(A+\alpha I)t}$, differentiating H and integrating over time in the interval $(0, \infty)$, we obtain

$$dH = -(A + \alpha I)^T H(t) - H(t)(A + \alpha I)$$

$$-H(0) = -(A + \alpha I)^T P - P(A + \alpha I)$$

and

$$(A + \alpha I)^T P + P(A + \alpha I) = QQ^T$$

2. Construct a Lyapunov function $V = \varepsilon^T P \varepsilon$ and compute its time derivative

$$V_t \le \varepsilon^T (A^T - QQ^T P^{-1}) P\varepsilon + \varepsilon^T P(A - P^{-1}QQ^T)\varepsilon + \frac{\beta\lambda_u}{\alpha - \alpha_m}\varepsilon^T\varepsilon$$

Adding and subtracting the term $2\alpha\varepsilon^T P\varepsilon$, and using Eq. A3, we obtain

$$V_t \le \varepsilon^T (A^T + \alpha I) P\varepsilon + \varepsilon^T P^T (A + \alpha I)\varepsilon - 2\varepsilon QQ^T\varepsilon - 2\alpha\varepsilon^T\varepsilon + \frac{\beta\lambda_u}{\alpha - \alpha_m}\varepsilon^T\varepsilon$$

$$V_t \le -\varepsilon QQ^T\varepsilon - 2\alpha\varepsilon^T P\varepsilon + \frac{\beta\lambda_u}{\alpha - \alpha_m}\varepsilon^T\varepsilon$$

$$V_t \le -\left[\lambda_l - \frac{\beta\lambda_u}{\alpha - \alpha_m}\right]\varepsilon^T\varepsilon \tag{A4}$$

On the other hand, because $\alpha > \alpha_m + \beta\lambda_u/[(1 - \eta)\lambda_l]$

$$\lambda_l - \frac{\beta\lambda_u}{\alpha - \alpha_m} > 0$$

and inequality A4 becomes

$$V_t \le -\eta\lambda_l\varepsilon^T\varepsilon$$

Finally, the result follows by making use of the well-known Gronwall–Bellman lemma (Khalil, 1996) to obtain

$$\|\varepsilon\|^2 \le \gamma_1\|\varepsilon_0\|^2 e^{-\eta\lambda_l t}$$

where γ_1 is an arbitrary constant.

Appendix B

To compute complete conditional sequences $\{\eta_i^{(p)}\}_{[a,b,c]}$, we start with a brief summary of an alternative notation for matrix and vector manipulation that will help us to simplify the algorithm description.

An index vector $a = [i:j]$ with $i < j$ is the sequence of all ordered integers between $i - 1$ and $j + 1$. Using this definition, we will represent any $n \times m$ matrix A by a pair of index vectors $[1:n]$ and $[1:m]$ as $A([1:n], [1:m])$. Whenever n and m are known explicitly or by the context, we will also use the short form $A(:, :)$. If $b \in Z^r$ (with $r < m$) is an arbitrary vector of given integers not larger than m, then $A(i, b)$ is a row vector with elements taken from the ith row of the matrix A at the columns given by b. Brackets "[ ]" will be also used to construct new vectors and matrices so that if A and B are $n \times m$ and $n \times k$ matrices, respectively, then $C = [A, B]$ is the corresponding $n \times (m + k)$ row block matrix with A and B as elements.

In addition let us include the following definitions:

(1) Sorting operations $i = \mathfrak{S}(u)$ over an arbitrary vector $u \in R^n$ are defined as those that give the sequence of indexes that sorts the elements of u in decreasing order. The equivalent in increasing order is denoted as $-i$.

(2) Given a vector $u \in R^n$ and an integer index matrix $A \in Z^{r\times s}$, with elements not larger than n, the operator $N = \mathfrak{N}(u, A)$ is defined as that which computes a matrix N with elements being elements of u in the order given by A, that is

$$\mathfrak{N}(u, A) = \begin{bmatrix} u[A(1, [1 : s])] \\ \vdots \\ u[A(r, [1 : s])] \end{bmatrix}$$

(3) Given a matrix $A \in R^{r\times s}$, with $A(i, j) = A(i - 1, j + 1)$ for all $i = 2, \ldots, r - 1$, and $j = 2, \ldots, s - 1$, the operator $u = \mathfrak{A}(A)$ (where $u \in R^{r+s-1}$) is defined as that which extracts the antidiagonal elements of A.

The algorithm to compute conditional decreasing sequences is based on the following simple fact:

Given a vector $\sigma \in (R^+)^n$, an index vector $\eta \in Z^r$ with elements taken from $I = [1 : n]$, and an integer m with $m < r < n$, then all possible r-sequences of η elements $\{\eta'^{(p)}\}$, with $\eta'^{(p)} \in Z^m$, satisfy

$$a \le \{\Im(\sigma, \eta'^{(p)})\} \le b$$

with

$$b = \Im(\sigma, i([1 : m])) \qquad a = \Im(\sigma, -i([1 : m])) \tag{B1}$$

and $i = \mathfrak{S}[\sigma(\eta)]$.

In what follows, and without loss of generality, we summarize the algorithm employed to compute a complete conditional sequence $\{\eta_1^{(p)}\}_{[a,b,c]}$, with $\eta_1^{(p)} \in Z^m$, for two given n-dimensional vectors (n m) σ_1 and σ_2 with positive real elements.

Algorithm description

1. Construct the $(n - m + 1) \times m$ matrix $N = \mathfrak{N}[\mathfrak{S}(\sigma_1), T]$, with T defined by the following expression

$$T = \begin{bmatrix} 1 & 2 & \cdots & m \\ 2 & 3 & \ddots & m + 1 \\ \vdots & \vdots & \ddots & \vdots \\ n - m + 1 & n - m + 2 & \cdots & n \end{bmatrix}$$

2. Set up $l = n - m + 1$, a matrix $M = [\varnothing]$ and set up integers $r = 1$, $s = 1$.

3. For given integers r (with $1 \le r \le m - 1$) and s (with $1 \le s \le l$) construct a matrix M_r^s as

$$M_r^s = \begin{bmatrix} N(s, [1 : r]) & \\ \vdots & N([s : l], [r + 1 : m]) \\ N(s, [1 : r]) & \end{bmatrix}$$

and compute

$$N_1 = \mathfrak{N}[\sigma_1, M_r^s] \qquad N_2 = \mathfrak{N}[\sigma_2, M_r^s]$$

$$u_1 = \mathfrak{A}[N_1(:, [r + 1 : m])] \qquad u_2 = \mathfrak{A}[N_2(:, [r + 1 : m])]$$

$$i_1 = \mathfrak{S}[u_1] \qquad i_2 = \mathfrak{S}[u_2]$$

4. Compute bounds as in Eq. B1.

$$b_s = \Im(u_1, i_1([1 : m - r])) + \Im(N_1(1, [1 : r]), [1 : r])$$

$$a_s = \Im(u_1, -i_1([1 : m - r])) + \Im(N_1(1, [1 : r]), [1 : r])$$

$$c_s = \Im(u_2, i_2([1 : m - r])) + \Im(N_2(1, [1 : r]), [1 : r])$$

- If $c_s < c$ or $b < a_s$ or $b_s < a$ set up $s = s + 1$ and go to step 3. If not, set up $M = [M, M_r^s]^T$, $N = M$, and $s = s + 1$ and go to step 3.
- If $s = l$, set up $N = M$ and $r = r + 1$ and go to step 3.
- If $r = m - 1$, stop. Matrix M will contain as rows the complete conditional sequence $\{\eta_1^{(p)}\}_{[a,b,c]}$.

Manuscript received Sep. 13, 2002, and revision received Aug. 23, 2003.